Crossover from Incoherent to Coherent Thermal Conduction in Bulk Titanium Oxide Natural Superlattices

Shunta Harada[1,2,3], Naoki Kosaka[2], Takashi Yagi[4,5], Shunya Sugimoto[2], Miho Tagawa[1,2], Toru Ujihara[1,2,6]*

[1] Center for Integrated Research of Future Electronics (CIRFE), Institute of Materials and Systems for Sustainability (IMaSS), Nagoya University, Furo-cho, Chikusa-ku, Nagoya 464-8601, Japan

[2] Department of Materials Process Engineering, Nagoya University, Furo-cho, Chikusa-ku, Nagoya 464-8603, Japan

[3] PRESTO, Japan Science and Technology Agency, 4-1-8 Honcho, Kawaguchi, Saitama 332-0012, Japan

[4] National Metrology Institute of Japan, National Institute of Advanced Industrial Science and Technology, Tsukuba, Ibaraki 305-8565, Japan

[5] CREST, Japan Science and Technology Agency, 4-1-8 Honcho, Kawaguchi, Saitama 332-0012, Japan

[6] GaN Advanced Device Open Innovation Laboratory (GaN-OIL), National Institute of Advanced Industrial Science and Technology (AIST), Nagoya University, Furo-cho, Chikusa-ku, Nagoya 464-8601, Japan

Keywords

coherent thermal conduction, natural superlattice, crystallographic shear structure

Abstract

We have investigated thermal conduction in bulk titanium oxide natural superlattices with crystallographic shear (CS) structures, in which dense planar faults are introduced with different periodicities, prepared by reductive annealing of rutile TiO_2 and crystal growth by the floating zone method. High-angle annular dark-field (HAADF) scanning transmission electron microscopy (STEM) revealed that $(132)_{rutile}$ and $(121)_{rutile}$ CS planes with interspacings of 2.7 and 1.0 nm were introduced in the mother rutile structure. Time-domain thermoreflectance (TDTR) revealed that the thermal conductivity decreased by the introduction of CS planes, but that the decrease is not monotonic with increasing density of CS planes. Calculation of the thermal conductivity and the mean free path for phonons revealed that a crossover from incoherent to coherent thermal conduction took place, and coherent interfaces with nanoscale periodicity were formed as thermodynamically stable phases in bulk titanium oxide natural superlattices.

Control of coherent thermal conduction by nanoscale periodic structures is of great interest for advanced thermal management, which differs from the diffusive picture that follows Fourier's law[1–8]. As is described in latter, the interfaces in crystalline materials such as artificial

superlattices are often behave as the source of diffuse scattering for thermal phonons due to its structural imperfection. While the perfect interfaces behave as the source of specular reflection of thermal phonons resulting in the modification of phonon dispersion by the zone-folding effects[9,10]. Here we call former case as “incoherent thermal conduction” and latter case as “coherent thermal conduction”. Coherent thermal conduction in nanostructures has been investigated in phononic crystals[3,11–13], artificial superlattice thin films[14–19] or other nanostructured materials[20–23]. Although phononic crystals successfully demonstrated the control of low-frequency phonons as well as heat conduction at liquid-helium temperature, it is necessary to achieve atomic-scale periodic structure with pristine interfaces for heat control, especially above room temperature. Artificial superlattices are the ideal system to investigate coherent thermal conduction. However, the imperfection of interfaces in artificial superlattices often hinders coherent thermal conduction, and the heat conduction through artificial superlattices was revealed to be mainly incoherent[24–27]. Despite the difficulty in obtaining perfect interfaces, some researchers have demonstrated coherent thermal conduction in artificial superlattices with their novel analyzing method and their superior technology in sample preparation. Luckyanova et al. reported coherent thermal conduction in AlAs/GaAs artificial superlattices with varying numbers of periods prepared by molecular beam epitaxy (MBE)[16]. Ravichandran et al. demonstrated crossover from incoherent to coherent thermal conduction, in which the thermal conductivity exhibits a minimum as a function of interface density, using epitaxial oxide superlattices grown by metal-organic chemical vapor deposition (MOCVD), with proper materials selection and a controlled growth process to make high-quality oxide superlattices with atomically sharp interfaces[18]. Saha et al. reported that thermal transport in TiN/(Al,Sc)N metal/semiconductor superlattices fabricated by dc-magnetron sputtering is dominated by phonon

wave effects[19]. Although interfaces with high structural perfection were reported to be achieved in the artificial superlattices, the realization of coherent interfaces for thermal phonons is still challenging. In order to obtain nanostructures with coherent interfaces, we focused on titanium oxide natural superlattices with crystallographic shear structures[28–30]. In our previous study, we reported that the interfaces in titanium oxide natural superlattices have pristine interfaces, and behave coherently for almost all phonons in rutile TiO_2[31]. In the present study, we investigated the thermal conduction in bulk titanium oxide natural superlattices as a function of the period of the coherent interfaces.

Three crystals were prepared for the measurement of thermal conductivity. One was a rutile TiO_2 single crystal grown by the Verneuil method purchased from Crystal Base Co. Ltd. (Osaka, Japan). Another was a reduced rutile crystal, which was prepared from a rutile TiO_2 single crystal by annealing at 1573 K for 24 h in vacuo ($<1\times10^{-4}$ Pa) with titanium metal ingots as oxygen getters. This reduced rutile crystal had a CS structure with (132) CS planes and was identical to a crystal for which we previously reported the atomic arrangement and structural perfection[31]. The other was a titanium-chromium oxide grown by the optical floating zone (FZ) method. Titanium-chromium oxide was reported to possess a CS structure with the direction and interspacing of CS planes dependent on the chromium concentration[32–37]. Commercial TiO_2 and Cr_2O_3 powders weighed in the proper ratio (Ti:Cr = 3:1) were mixed in a zirconia mortar and pressed to form a bar shape by an isostatic pressing machine. Then, the pressed bars were sintered at 1273 K for 24 hours. The sintered ceramics were used as the seed and feed for a crystal grown by the FZ method at a growth rate of 2.5 mm/h under an argon flow. The atomic structure was examined by transmission electron microscopy (TEM) as well as high-angle annular dark field (HAADF)

scanning transmission electron microscopy (STEM) using a JEOL JEM-ARM200 transmission electron microscope operated at 200 kV.

The orientation of the crystals was determined by the back-reflection Laue method as well as the electron backscatter diffraction (EBSD) method using a PHI 700Xi (ULVAC, Inc.). After orientation determination, the crystals were cut by a low-speed wheel saw and polished by diamond slurries with particle sizes of 9, 3, and 1 μm.

The thermal conductivity of the crystals was measured by a time-domain thermoreflectance (TDTR) apparatus[38–42]. A Mo layer with a thickness of 100 nm was deposited on the polished crystals by dc magnetron sputtering. The repetition rate, modulation frequency, wavelength and spot diameter of the pump laser were 20 MHz, 200 kHz, 1550 nm and 50 μm, respectively, and those of the probe laser were 20 MHz, 775 nm and 25 μm, respectively. Thermal diffusivity was evaluated from fitting of the measured thermoreflectance signals, and the thermal conductivity was estimated from the reported specific heat for rutile TiO_2[43]. TDTR measurements were conducted at temperatures ranging from 123 to 573 K.

Figure 1 shows selected area electron beam diffraction (SAED) patterns obtained from the reduced rutile and titanium-chromium oxide crystals. A line of superlattice spots is directed along $(132)_{rutile}$ and $(121)_{rutile}$ in the SAED patterns obtained from the reduced rutile and titanium-chromium oxide, respectively. The interval of the superlattice spots for reduced rutile (Fig. 1(a)) corresponds to 26 times the $(132)_{rutile}$ interplanar spacing. As also described in Ref. 29, although different periodicities including 26, 27 and 28 times the interplanar spacing of $(132)_{rutile}$ were observed, the superlattice spots were sharp and no streaks were noticed. The interval of superlattice spots shown in Fig. 1(b) for titanium-chromium oxide corresponded to 6 times the $(121)_{rutile}$

interplanar spacing and the superlattice spots exhibited streaking. At other positions, an 8-times periodicity was also observed. It seems that the structure was not homogeneous and had disorder in the periodicity of the $(121)_{rutile}$ CS planes. Recently, Anderson localization of phonons in aperiodic superlattices with large degree of randomness was reported[44], which would leads to the reduction of thermal conductivity. Now we are trying to control the disorder in the periodicity of the CS planes by heat treatment and investigating the effect of aperiodicity. The direction and the interplanar spacing of CS planes (D_{CS}) estimated from the SAED patterns are summarized in Table I.

Figure 2 shows HAADF-STEM images taken from the natural superlattice crystals. In the HAADF-STEM images, cation (Ti^{4+}, Ti^{3+} and/or Cr^{3+}) columns are imaged as bright spots, while anion (O^{2-}) columns are not imaged individually. The arrangement of the cation columns deviates on the $(132)_{rutile}$ and $(121)_{rutile}$ CS planes for the reduced rutile and the titanium-chromium oxide, respectively. From the HAADF-STEM observations, the interplanar spacings of the CS planes can be evaluated by counting the number of $(132)_{rutile}$ and $(121)_{rutile}$ layers (n), and the value of n was evidently 26 and 6, respectively, although the number of layers sometimes varied, especially in the titanium-chromium oxide. Considering the nominal composition of the titanium-chromium (Ti:Cr = 3:1) oxide, one can expect the occurrence of 8-fold periodicity in for $(121)_{rutile}$ planes for the $Cr_2Ti_6O_{15}$ ($Cr_{0.25}Ti_{0.75}O_{1.875}$) phase. The current results indicate that additional oxygen deficiency was created due to reduction during FZ crystal growth under an argon atmosphere. If the periodicity is strictly 6-fold and chromium evaporation is negligible, the chemical formula can be expressed as $(Cr_{0.25}Ti_{0.75})_6O_{11}$ ($Cr_{0.25}Ti_{0.75}O_{1.833}$).

Figure 3 shows the temperature dependence of the thermal conductivity along the $[100]_{rutile}$ direction evaluated from TDTR measurements. The thermal conductivity for rutile TiO_2 decreases

with increasing temperature, in good agreement with the previously reported values by Thurber and Mante from measurements using a static method[45]. The thermal conductivity for the crystals with CS structures was lower than that for the rutile crystal below room temperature and almost the same above room temperature. Note that the thermal conductivity for the reduced rutile crystal is lower than that for the titanium-chromium oxide crystal, although the density of CS planes for the reduced rutile was lower than that of the titanium-chromium oxide crystal, which was apparent especially at low temperatures. Since electrical contribution of thermal conductivity for these CS phases was expected to be negligibly small from the literatures [46,47], the current results represent the characteristic of the phonon thermal conduction.

In order to evaluate the incoherent aspect of thermal conduction in the prepared crystals, we calculated the thermal conductivity using a Debye-Callaway model as follows:

$$K = \frac{1}{3}\int_0^{\omega_D} \tau(\omega) C(\omega) v^2 d\omega \quad (1)$$

where K, ω_D, $\tau(\omega)$, $C(\omega)$ and v represent the thermal conductivity, Debye cut-off frequency, relaxation time and specific heat sound velocity, respectively. The relaxation time is given by Matthiessen's rule:

$$\tau(\omega)^{-1} = \tau_b(\omega)^{-1} + \tau_i(\omega)^{-1} + \tau_u(\omega)^{-1}\,, \quad (2)$$

$$\tau_b(\omega)^{-1} = \frac{v}{L}, \quad (3)$$

$$\tau_i(\omega)^{-1} = A\omega^4, \quad (4)$$

$$\tau_u(\omega)^{-1} = B_1\omega^2 T e^{-B_2/T}, \quad (5)$$

where τ_b, τ_i and τ_u are the relaxation times for boundary scattering, impurity scattering and Umklapp scattering, respectively, and L, T, A, B_1 and B_2 are the boundary length, temperature, and constants for impurity scattering and Umklapp scattering, respectively. The formulas for the relaxation times used in this calculation are identical to those reported by Thurber and Mante[45]. Here, we assumed to neglect the effect of the change in impurity scattering due to the Cr addition and Umklapp scattering by the difference in unit cell volume. Since the difference in atomic mass is less than 10%, change in the impurity scattering is expected to be small. Umklapp scattering becomes significant above the Debye temperature, of which titanium oxide is as high as 760 K. Furthermore, the thermal conductivity of the specimen with CS planes was almost independent of temperature, which implies that the thermal conduction is not limited by Umklapp scattering as was also discussed in the system of tungsten oxides with CS structure[48]. Although phonon-frequency dependent relaxation time of boundary scattering was reported [16], in the present calculation model for incoherent thermal conduction, we simply assume a boundary scattering length (L) that is equal to the interspacing of the CS planes for the reduced rutile and the titanium-chromium oxide as tabulated in Table I, and the other parameters are assumed to be identical to those reported in Ref. 41. Figure 4 shows the thermal conductivity values determined from TDTR measurements, as well as those calculated by the incoherent Debye-Callaway model as a function of the density of CS planes (inverse of the interspacing of CS planes) at 173, 298 and 473 K. Although the incoherent model partly reproduces the experimental results in which the thermal conductivity decreases by the introduction of CS planes, especially at low temperature (below RT), the increase in thermal conductivity with increasing density of CS planes could not be accounted for by this incoherent model.

Assuming the Debye model, the mean free path for phonons can be estimated for a single crystal of rutile TiO_2 along the $[100]_{rutile}$ direction using the following equation and measured thermal conductivity,

$$\lambda_{lattice} = \frac{1}{3} C_p \rho v l \qquad (6)$$

where C_p and v stand respectively for the specific heat and sound velocity, and l is the mean free path for phonons. The values of the mean free path for phonons estimated by Eq. (6) at each temperature are also shown in Fig. 4, and suggest that deviation from the calculated thermal conductivity using the incoherent model will become apparent when the interspacing of CS planes is smaller than the mean free path except at high temperature (above RT), because the Debye-Callaway model is valid at low temperatures (below RT). The incoherent model seems to partly account for the decrease in thermal conductivity when the mean free path is smaller than the interspacing of CS planes. The deviation from incoherent model when the mean free path is larger than the interspacing of CS planes implies that the thermal conduction mechanism changes to coherent as was discussed in ref. [2,18]. The present results indicate that a crossover from incoherent to coherent thermal conduction[18,49] takes place in bulk titanium oxide natural superlattices with CS structures, especially at lower temperatures. Further theoretical investigation would elucidate the detail of the coherent thermal conduction mechanism including zone-folding of phonon bands, which was not considered in the present discussion, in the natural superlattice bulk crystals.

The present result that coherent thermal conduction emerges also indicates that the interfaces introduced in the CS structure behave as coherent interfaces with high structural perfection, as expected from the HAADF-STEM observations in the present study as well as in

our previous report[31,37]. In other words, the structural perfection of the interfaces in titanium oxide natural superlattices can be estimated with some accuracy from the HAADF-STEM observations.

In conclusion, we have observed crossover from incoherent to coherent thermal conduction in bulk titanium oxide natural superlattice crystals with CS structures having different periodicities prepared by reductive annealing and FZ crystal growth. As expected from HAADF-STEM observations of an almost perfect atomic arrangement of CS planes, the interfaces in the crystals behave as coherent interfaces for thermal phonons, and coherent thermal conduction becomes apparent. Considering the tunability of the periodicity and the structural perfection[37], titanium oxide natural superlattices are an ideal system for the investigation of the details of coherent thermal conduction in nanoscale periodic structures. Furthermore, the demonstration of coherent thermal conduction in bulk materials points the way toward advanced heat control by harnessing the wave nature of phonons, which are difficult to prepare by conventional processes such as those used for the preparation of artificial superlattice thin films.

AUTHOR INFORMATION

Corresponding Author

*Shunta Harada

Institute of Materials and Systems for Sustainability, Nagoya University, Furo-cho, Chikusa-ku, Nagoya, 464-8601 Japan; E-mail: shunta.harada@nagoya-u.jp

Author Contributions

S. H. conceived and designed the experiments. N. K. mainly conducted the experiments and the analysis with S. S. under the guidance of S. H. TDTR measurements were conducted by N. K. with T. Y. HAADF-STEM observations and structural analyses were conducted by S. H. The experimental data and analysis were discussed by all authors. The manuscript was written by S. H based on the manuscript prepared by N. K. All authors have given approval for the final version of the manuscript.

Note

The authors declare no competing financial interest.

ACKNOWLEDGMENT

This work was supported in part by JST PRESTO grant (JPMJPR18I8), a Grant-in-Aid for Scientific Research (B) from MEXT (18H01733) and JST CREST grant (JPMJCR17I2).

REFERENCES

[1] V. Narayanamurti, Science 213 (1981) 717–723.

[2] M. V. Simkin, G.D. Mahan, Phys. Rev. Lett. 84 (2000) 927–930.

[3] J.K. Yu, S. Mitrovic, D. Tham, J. Varghese, J.R. Heath, Nat. Nanotechnol. 5 (2010) 718–721.

[4] E. Dechaumphai, R. Chen, J. Appl. Phys. 111 (2012).

[5] M. Maldovan, Nature 503 (2013) 209–217.

[6] M. Maldovan, Nat. Mater. 14 (2015) 667–674.

[7] M. Nomura, J. Shiomi, T. Shiga, R. Anufriev, Jpn. J. Appl. Phys. 57 (2018) 080101.

[8] Y. Liao, T. Shiga, M. Kashiwagi, J. Shiomi, Phys. Rev. B 98 (2018) 134307.

[9] A. Yamamoto, T. Mishina, Y. Masumoto, M. Nakayama, Phys. Rev. Lett. 73 (1994) 740.

[10] E. Dechaumphai, R. Chen, J. Appl. Phys. 111 (2012) 073508.

[11] S. Alaie, D.F. Goettler, M. Su, Z.C. Leseman, C.M. Reinke, I. El-Kady, Nat. Commun. 6 (2015) 8228.

[12] M.R. Wagner, B. Graczykowski, J.S. Reparaz, A. El Sachat, M. Sledzinska, F. Alzina, C.M. Sotomayor Torres, Nano Lett. 16 (2016) 5661–5668.

[13] J. Maire, R. Anufriev, R. Yanagisawa, A. Ramiere, S. Volz, M. Nomura, Sci. Adv. 3 (2017) e1700027.

[14] B. Yang, G. Chen, Phys. Rev. B 67 (2003) 195311.

[15] Y.K. Koh, Y. Cao, D.G. Cahill, D. Jena, Adv. Funct. Mater. 19 (2009) 610–615.

[16] M.N. Luckyanova, J. Garg, K. Esfarjani, A. Jandl, M.T. Bulsara, A.J. Schmidt, A.J. Minnich, S. Chen, M.S. Dresselhaus, Z. Ren, E.A. Fitzgerald, G. Chen, Science 338 (2012) 936–939.

[17] M.N. Luckyanova, J.A. Johnson, A.A. Maznev, J. Garg, A. Jandl, M.T. Bulsara, E.A. Fitzgerald, K.A. Nelson, G. Chen, Nano Lett. 13 (2013) 3973–3977.

[18] J. Ravichandran, A.K. Yadav, R. Cheaito, P.B. Rossen, A. Soukiassian, S.J. Suresha, J.C. Duda, B.M. Foley, C.H. Lee, Y. Zhu, A.W. Lichtenberger, J.E. Moore, D.A. Muller, D.G. Schlom, P.E. Hopkins, A. Majumdar, R. Ramesh, M.A. Zurbuchen, Nat. Mater. 13 (2014) 168–172.

[19] B. Saha, Y.R. Koh, J.P. Feser, S. Sadasivam, T.S. Fisher, A. Shakouri, T.D. Sands, J. Appl. Phys. 121 (2017) 015109.

[20] M.C. Wingert, Z.C.Y. Chen, E. Dechaumphai, J. Moon, J.H. Kim, J. Xiang, R. Chen, Nano Lett. 11 (2011) 5507–5513.

[21] J. Chen, G. Zhang, B. Li, Nano Lett. 12 (2012) 2826–2832.

[22] M.N. Luckyanova, J. Mendoza, H. Lu, B. Song, S. Huang, J. Zhou, M. Li, Y. Dong, H. Zhou, J. Garlow, L. Wu, B.J. Kirby, A.J. Grutter, A.A. Puretzky, Y. Zhu, M.S. Dresselhaus, A. Gossard, G. Chen, Sci. Adv. 4 (2018) eaat9460.

[23] T. Taniguchi, T. Terada, Y. Komatsubara, T. Ishibe, K. Konoike, A. Sanada, N. Naruse, Y. Mera, Y. Nakamura, Nanoscale 13 (2021) 4971–4977.

[24] T. Yao, Appl. Phys. Lett. 51 (1987) 1798–1800.

[25] X.Y. Yu, G. Chen, A. Verma, J.S. Smith, Appl. Phys. Lett. 67 (1995) 3554.

[26] W.S. Capinski, H.J. Maris, T. Ruf, M. Cardona, K. Ploog, D.S. Katzer, Phys. Rev. B 59 (1999) 8105–8113.

[27] S.M. Lee, D.G. Cahill, R. Venkatasubramanian, Appl. Phys. Lett. 70 (1997) 2957–2959.

[28] S. Andersson, B. Collén, U. Kuylenstierna, A. Magnéli, Acta Chem. Scand. 11 (1957) 1641–1652.

[29] Y. Le Page, P. Strobel, J. Solid State Chem. 44 (1982) 273–281.

[30] S. Harada, K. Tanaka, H. Inui, J. Appl. Phys. 108 (2010) 083703.

[31] S. Harada, N. Kosaka, M. Tagawa, T. Ujihara, J. Phys. Chem. C 125 (2021) 11175–11181.

[32] S. Andersson, A. Sundholm, A. Magnéli, B. Högberg, P. Kneip, H. Palmstierna, Acta Chem. Scand. 13 (1959) 989–997.

[33] O.W. Flörke, C.W. Lee, J. Solid State Chem. 1 (1970) 445–453.

[34] L.A. Bursill, B.G. Hyde, D.K. Philp, Philos. Mag. 23 (1971) 1501–1513.

[35] R.M. Gibb, J.S. Anderson, J. Solid State Chem. 4 (1972) 379–390.

[36] S. Somiya, S. Hirano, S. Kamiya, J. Solid State Chem. 25 (1978) 273–284.

[37] S. Harada, S. Sugimoto, N. Kosaka, M. Tagawa, T. Ujihara, J. Phys. Chem. C 125 (2021) 15730–15736.

[38] C.A. Paddock, G.L. Eesley, J. Appl. Phys. 60 (1986) 285–290.

[39] N. Taketoshi, T. Baba, A. Ono, Meas. Sci. Technol. 12 (2001) 2064–2073.

[40] N. Taketoshi, T. Baba, A. Ono, Rev. Sci. Instrum. 76 (2005) 094903.

[41] T. Yagi, K. Tamano, Y. Sato, N. Taketoshi, T. Baba, Y. Shigesato, J. Vac. Sci. Technol. A 23 (2005) 1180–1186.

[42] Y. Yamashita, K. Honda, T. Yagi, J. Jia, N. Taketoshi, Y. Shigesato, J. Appl. Phys. 125 (2019) 35101.

[43] S.J. Smith, R. Stevens, S. Liu, G. Li, A. Navrotsky, J. Boerio-Goates, B.F. Woodfield, Am. Mineral. 94 (2009) 236–243.

[44] T. Juntunen, O. Vänskä, I. Tittonen, Phys. Rev. Lett. 122 (2019) 105901.

[45] W.R. Thurber, A.J.H. Mante, Phys. Rev. 139 (1965) A1655.

[46] K.M. Ok, Y. Ohishi, H. Muta, K. Kurosaki, S. Yamanaka, J. Am. Ceram. Soc. 101 (2018) 334–346.

[47] E. Tani, J.F. Baumard, J. Solid State Chem. 32 (1980) 105–113.

[48] G. Kieslich, U. Burkhardt, C.S. Birkel, I. Veremchuk, J.E. Douglas, M.W. Gaultois, I. Lieberwirth, R. Seshadri, G.D. Stucky, Y. Grin, W. Tremel, J. Mater. Chem. A 2 (2014) 13492–13497.

[49] H.J. Cho, Y. Wu, Y. Zhang, B. Feng, M. Mikami, W. Shin, Y. Ikuhara, Y. Sheu, K. Saito, H. Ohta, Adv. Mater. Interfaces 8 (2021) 2001932.

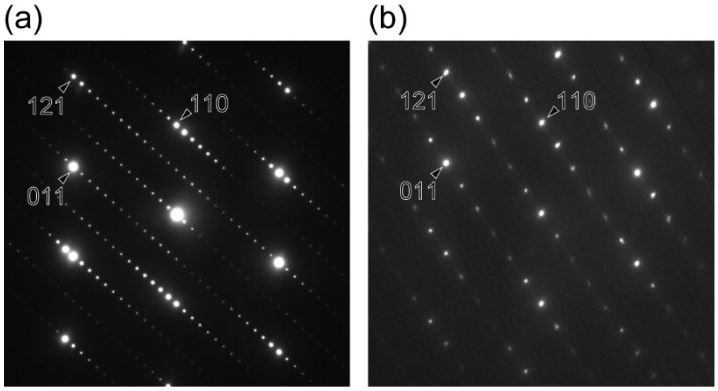
(a)
121
110
011
(b)
121
110
011

Table I. Direction and interspacing of CS planes estimated from SAED patterns for the reduced rutile crystal and the titanium-chromium oxide crystal.

Specimen	CS plane	n	D_{CS} (nm)
Reduced rutile	$(132)_{rutile}$	26-28	2.6-2.9
Titanium-chromium oxide (FZ)	$(121)_{rutile}$	6-8	0.95-1.3

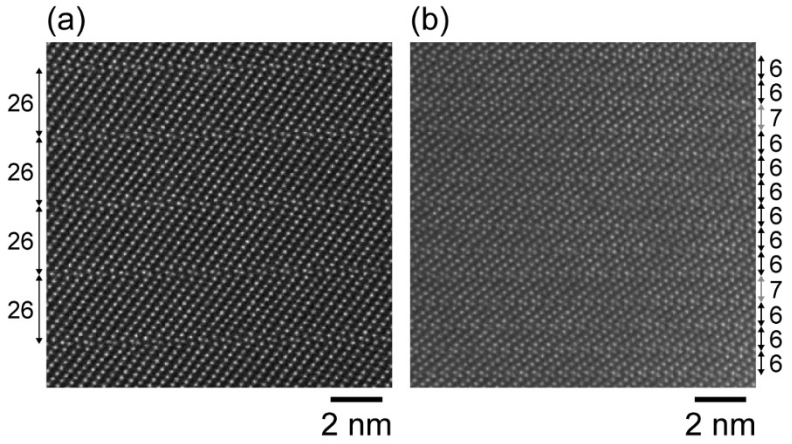

Figure 2. (a) HAADF-STEM image of reduced rutile along the $[1\text{-}11]_{rutile}$ zone axis. $(132)_{rutile}$ CS planes were periodically introduced into the mother rutile crystal, corresponding to n = 26. (b) HAADF-STEM image for the titanium-chromium oxide crystal along the $[1\text{-}11]_{rutile}$ zone axis. $(121)_{rutile}$ CS planes were periodically introduced into the mother rutile crystal, corresponding to n = 6 for the most part, but with occasional changes in periodicity (n = 7).

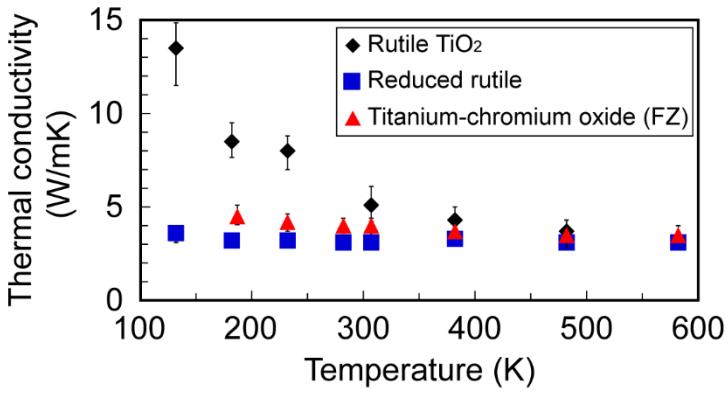

Figure 3. Thermal conductivity of rutile TiO_2, the reduced rutile crystal and the titanium-chromium oxide crystal along the $[100]_{rutile}$ direction measured by TDTR.

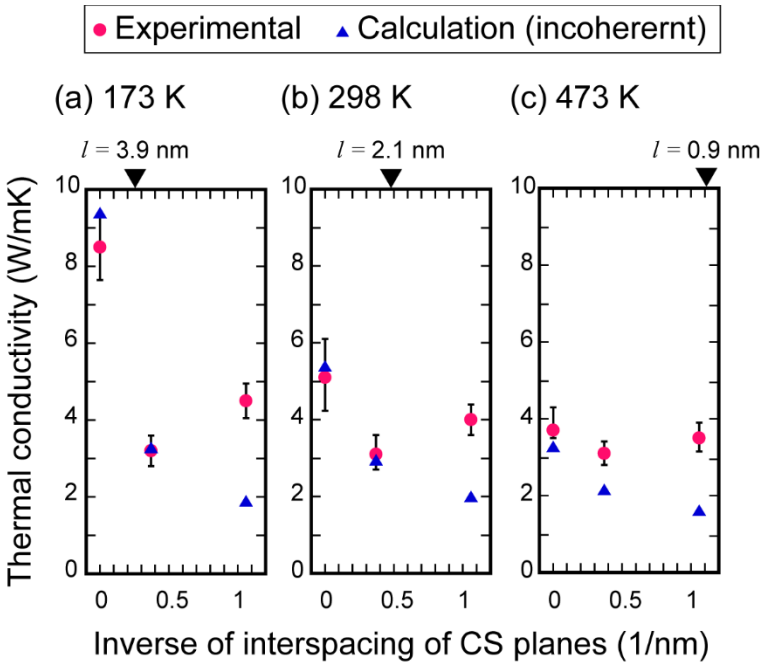

Figure 4. Thermal conductivity determined from TDTR measurements and calculated using the incoherent Debye-Callaway model as a function of the density of CS planes (inverse of the interspacing of CS planes) at 173, 298 and 473 K. The values of the mean free path for phonons (l) estimated by Eq. (6) at each temperature are also shown.

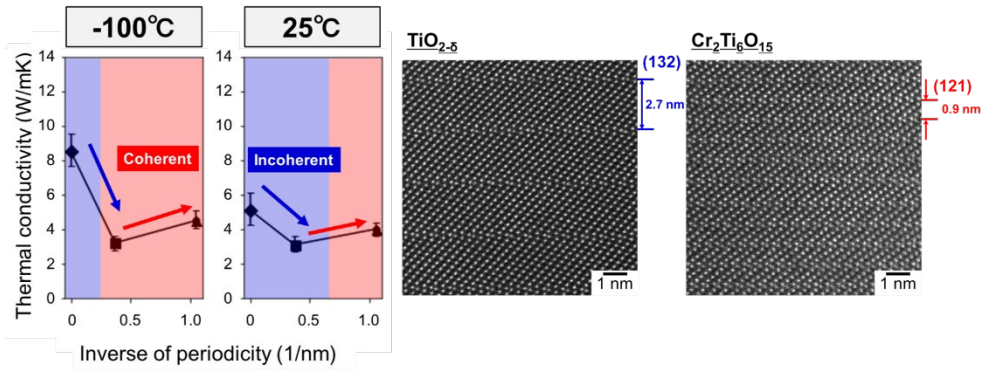

Graphical abstract